Published in final edited form as:
J Mol Biol. 2008 October 24; 382(5): 1136–1143. doi:10.1016/j.jmb.2008.07.089.

EVIDENCE AGAINST INVOLVEMENT OF AQUAPORIN-4 IN CELL-CELL ADHESION

Hua Zhang and **A. S. Verkman**
Departments of Medicine and Physiology, University of California, San Francisco CA 94143-0521, U.S.A

Summary

Aquaporin-4 (AQP4) water channels are expressed strongly in glial cells, where they play a role in brain water balance, neuroexcitation and glial cell migration. Here, we investigated a proposed new role of AQP4 in facilitating cell-cell adhesion. Measurements were made in differentiated primary glial cell cultures from wildtype vs. AQP4 knockout mice, and in null vs. AQP4-transfected L-cells, a cell type lacking endogenous adhesion molecules, and in null vs. AQP4-transfected CHO-K1 cells and FRT cells. Using established assays of cell-cell adhesion, we found no significant effect of AQP4 expression on adhesion in each of the cell types. As a positive control, transfection with E-cadherin greatly increased cell-cell adhesion. High-level AQP4 expression also did not affect aggregation of plasma membrane vesicles in a sensitive quasi-elastic light scattering assay. Further, we found no specific AQP4 binding of a fluorescently labeled oligopeptide containing the putative adhesion sequence in the second extracellular loop of AQP4. These data provide evidence against involvement of AQP4 in cell-cell adhesion.

Keywords

cell adhesion; water channel; AQP4; glial cells; transgenic mice

Introduction

Aquaporin-4 (AQP4) is a water-selective transport protein expressed in plasma membranes in glial cells throughout the central nervous system. At least three distinct roles of AQP4 in brain physiology have been demonstrated [1]. AQP4 facilitates water movement into and out of the brain in a variety of pathological conditions such as water intoxication, stroke, infection, tumor and hydrocephalus [2–5], by facilitating osmotically driven water movement across barriers separating brain parenchyma and the blood and cerebrospinal fluid compartments. AQP4 increases the migration of glial cells in culture and in vivo models [6, 7], by a mechanism that likely involves facilitated water influx into lamellipodia at the leading edge of migrating cells [8]. AQP4 also modulates neuroexcitation phenomena, including seizure activity, cortical spreading depression, and visual, auditory and olfactory signal transduction [9–13], by a mechanism that may involve altered extracellular space volume and potassium buffering [11, 14].

Correspondence to: Alan S. Verkman, M.D., Ph.D., 1246 Health Sciences East Tower, University of California, San Francisco, CA 94143-0521, U.S.A. Phone: (415) 476-8530; Fax: (415) 665-3847 , Alan.Verkman@ucsf.edu; http:/www.ucsf.edu/verklab.

Recently, an interesting new role of AQP4 in facilitating cell-cell adhesion was proposed, based on structural data from 2-dimensional crystals in which an extracellular helix-helix interaction (at residues 139-142) was predicted [15]. The authors also reported increased clustering of L-cells following AQP4 transfection. Another study showed increased cell adhesion to various substrates when AQP4 was transfected into glioma cell lines [16]. There is also evidence that a related aquaporin, the major intrinsic protein of lens fiber (also called AQP0) facilitates adhesion of lens fiber cells in the eye [17, 18]. As reviewed recently [19], AQP4-dependent cell-cell adhesion could be important in brain development, blood-brain barrier integrity, and osmosensing. However, arguing against this speculation is the absence of such abnormalities in transgenic mice lacking AQP4 [1].

Here, we tested the potential role of AQP4 in cell-cell adhesion. We used primary glial cell cultures from wildtype vs. AQP4 knockout mice, null vs. AQP4-transfected L-cells, which lack endogenous adhesion molecules, and two other cell types in which transfection produces high levels of AQP4 expression. Utilizing established and novel assays of cell-cell adhesion, we found no evidence for AQP4-facilitated adhesion. Our conclusion that AQP4 residues 139–142 is not involved in adhesion was further supported by binding measurements of a peptide containing the putative adhesion sequence.

Results

Initial adhesion studies were done using L-cells, which lack endogenous adhesion molecules such as cadherin or N-CAM. Some experiments were done on stably transfected L-cells expressing AQP4. As shown in Fig. 1A, AQP4 was expressed in a plasma membrane pattern in the transfected cells with uniform cell-to-cell expression. Experiments were also done in control (non-transfected) L-cells, and in L-cells that were transiently transfected with AQP4 or E-cadherin (positive aggregation control [20]). Transient transfection produced high level AQP4 expression in ~60% of cells.

Cell aggregation was measured using a standard adhesion assay in which a cell suspension was stirred for specific times, and the number of particles (cells + cell aggregates) counted. Increased adhesion is seen as a reduction over time in the total number of particles. Fig. 1B shows the number of L-cell particles at 30 and 60 min. There was a small reduction in particle counts with time, though not different between non-transfected, stably transfected and transiently AQP4 transfected cells. Similar results were found in 3 sets of measurements on separate cell cultures. In the positive control, greatly increased adhesion (reduced particle count) was seen after L-cell transfection with E-cadherin. Fig. 1C shows light micrographs of the L-cells after glutaraldehyde (to freeze aggregation state) and settling onto a coverglass. Little aggregation was seen in non-transfected and AQP4-expressing L-cells, whereas many aggregates were seen in the E-cadherin-expressing L-cells. Similar aggregation studies done twice using control vs. AQP4 stably expressing CHO and FRT cells (generated previously as described [21, 22]) also showed no AQP4-dependent aggregation (data not shown).

AQP4 is expressed highly in brain glial cells, the most relevant cell type where AQP4-dependent cell adhesion might occur. Similar cell-cell adhesion measurements were done on cultured, differentiated glial cells having high AQP4 expression (Fig. 2A) and osmotic water permeability [23]. More than 90% of the cultured glial cells were GFAP positive and showed the characteristic stellate morphology. Particles (cells + cell aggregates) were counted following suspension in standard HBSS and Ca^{2+}/Mg^{2+}-free HBSS containing 10 mM EDTA. Fig. 2B shows greater baseline adhesion of the astrocytes than that seen for L-cells, though no difference in cultures from wildtype vs. AQP4 null mice. Elimination of calcium reduced adhesion, but still no difference was seen in cultures from wildtype vs. AQP4 null

mice. Fig. 2C shows micrographs of glial cells after settling onto a coverglass. Though distinct cell aggregates were seen, their numbers and appearance were similar in the cultures from wildtype and AQP4 null mice.

As another sensitive approach to detect adhesion of AQP4-expressing cells, we imaged glial cell aggregates following fluorescent labeling, with cells from wildtype mice labeled red and from AQP4 null mice labeled green. We previously established, for in vivo cell migration studies, fluorescence labeling procedures to stain cells brightly without effect on cell function [6]. We reasoned that cell aggregates, after mixing equal numbers of red and green cells, would be enriched in red cells if AQP4 enhanced cell-cell adhesion. Fig. 3A shows representative low magnification phase-contrast and fluorescence micrographs of cells/aggregates after a 30 min incubation in stirred suspension, showing comparable numbers of red and green cells, with both colors seen in aggregates. At high magnification the aggregates were seen to contain both red and green cells in an apparently random clustering (Fig. 3B, inset). To quantify the results, the numbers of red and green cells were counted in clusters containing at least 6 distinct cells. As summarized in Fig. 3B by a histogram of red/green cell counts, a statistical distribution as found, as expected, which was centered at a red/green ratio of unity for both cell types. These results indicate random, AQP4-independent glial cell adhesion. Similar results were found at 60 min (not shown).

We also studied binding to AQP4 of the putative AQP4 adhesion sequence. Differentiated glial cells or stably transfected AQP4-expressing CHO-K1 cells [22] were used. These cell types strongly express AQP4 in orthogonal arrays of particles [22, 24]. Binding was measured by quantitative imaging of confluent cell layers following incubation with a fluorescein-labeled 9-mer peptide containing extracellular loop residues of AQP4 proposed to mediate cell-cell adhesion (Fig. 4A, top). Inclusion of an excess of unlabeled peptide was used to detect specific binding. Fig. 4A (bottom) shows fluorescence micrographs of glial cells after incubations with fluorescent peptide in the absence and presence of a 50-fold excess of unlabeled peptide. Cells were then briefly fixed and washed prior to imaging. Though incubation with peptide increased fluorescence above background, fluorescence was similar in the cells from wildtype and AQP4 null mice, and when excess unlabeled peptide was present. Fig. 4C summarizes results from a series of measurements done at different concentrations of the fluorescent peptide in glial and CHO cells. No specific peptide binding was found based on similar fluorescence without vs. AQP4 at each concentration of fluorescent peptide, and by the lack of competition with a large excess of unlabeled peptide. These data show no specific association of the putative AQP4 adhesion sequence with the external-facing surface of AQP4 in cell membranes.

Last, as potentially the most sensitive test of AQP4-facilitated membrane adhesion, we measured aggregation of small plasma membrane vesicles (diameter ~ 200 nm) that strongly expressed AQP4 vs. control, non-expressing vesicles. Vesicles were prepared by homogenization and density gradient centrifugation of control and AQP4-expressing CHO cells, as done previously [22]. After shaking in standard HBSS overnight at high density, ~5 % of particles were aggregates with diameters greater than 2000 nm, for both control and AQP4-expressing vesicles. As positive controls, nearly all vesicles were contained in aggregates when a low-ionic strength sucrose buffer was used in place of HBSS during the incubation.

Discussion

Our data provide evidence against the involvement of AQP4 in cell-cell adhesion and the proposal that AQP4 serves as an ‘adhennel’ [19] with dual transport and adhesion roles. We found by multiple assays no evidence for increased adhesion/aggregation in cells expressing

AQP4 than in the same cell types not expressing AQP4, including the most relevant cell type, brain glial cells. Also, specific AQP4 binding was not seen of a peptide corresponding to the second extracellular domain of AQP4 with its putative adhesion sequence. As a negative study, however, we cannot exclude the possibility that under some conditions extracellular AQP4-AQP4 interactions can occur, though we are doubtful in part because of the absence of any of the predicted adhesion defects in AQP4-deficient mice.

The evidence for possible involvement of AQP4 in cell-cell adhesion came from structural analysis of double-layered 2-dimensional crystals of recombinant AQP4 [15]. Notwithstanding the limited structural resolution (3.2 Angstroms) and the variable orientations and distances between the two layers, it was found that apposing AQP4 monomers interacted at residues 139 and 142, located in their second extracellular loops. However, unlike the precise stacking of AQP0 in crystals [17, 18], the AQP4 crystals were offset such that tetramers in one membrane line overlay the center of tetramers in the apposing membrane. The crystallography data provide no information about the strength of the AQP4-AQP4 interaction or whether it occurs in real hydrated membranes or cells. If such interactions do occur in cells, it was speculated that the interactions might serve to block AQP4 water permeability and that rapid water flow might force interacting membranes apart.

Different cell types utilize different adhesion mechanisms. Well-characterized cell adhesion molecules include cadherins, immunoglobulin (Ig) superfamily molecules, and integrins, which perform a wide range of functions at cell contacts such as embryogenesis, immune response, hemostasis, inflammation, and maintenance of tissue integrity (reviewed in refs. 25 and 26). Cadherins are single-pass transmembrane glycoproteins with calcium-dependent adhesion, whereas adhesion in Ig superfamily molecules is calcium-independent. Cadherins and Ig molecules can form homophilic adhesion, whereas integrins are heterodimeric transmembrane glycoproteins that interact mainly with the extracellular matrix [27]. The mouse fibroblast L-cell is a good model to study cell adhesion because it expresses few if any adhesion molecules and shows little aggregation in standard cell aggregation assays [28–30]. We did not find increased aggregation of L-cells upon transient or stable AQP4 transfection, whereas E-cadherin expression increased aggregation.

From the crystal structure data, it was suggested each AQP4 tetramer interacts with four tetramers in the opposing membrane, such that AQP4 orthogonal arrays might enhance AQP4-facilitated adhesion [19]. The various cell types studied here express AQP4 in square, orthogonal arrays [22, 31]. Various aggregation assays on these cells, including a highly sensitive vesicle aggregation assay, showed no AQP4 dependence.

Because AQP4 is expressed mainly in brain glial cells, we studied the possibility of AQP4-dependent aggregation in cultured, differentiated glial cells. Glial cells are known to express several adhesion molecules, including the Ca^{2+}-dependent adhesion molecule N-cadherin [32], and the Ca^{2+}-independent Ig superfamily molecule nectin-1 [25]. Our data confirmed Ca^{2+}-dependent and independent adhesion of cultured glial cells. However, no differences in aggregation were found, using two different assays, in glial cells cultured from brains of wildtype vs. AQP4 null mice. These data support the conclusion that molecules other than AQP4 are responsible for glial cell-cell adhesion.

Finally, in peptide competition studies we were unable to detect specific AQP4 binding of the putative 3^{10} α-helix containing AQP4 residues 139–142. These results suggest that residues in the synthetic peptide have little or no affinity to the extracellular AQP4 surface. In a study of AQP4 membrane diffusion reported recently [33], we studied a rAQP4M23 construct containing a c-myc between residues 139 and 142, which serendipitously destroys the 3^{10} α-helix. The cellular processing, water permeability and ability to form orthogonal

arrays of this construct were not different from those of native (untagged) AQP4, providing further support for the conclusions here.

In summary, our data do not support the involvement of AQP4 in cell-cell adhesion, which would have ascribed two completely unrelated roles to AQP4. The well-documented water transporting role of AQP4 probably accounts for its various functions in brain water transport, glial cell migration, and neuroexcitation.

Materials and Methods

Cells and tranfection

Mouse fibroblast L-cells (ATCC CCL-1) were cultured in MEM supplemented with 10% FBS, 100 U/ml penicillin and 100 μg/ml streptomycin under 5% CO_2 at 37 °C. L-cells were transfected with rat AQP4 (rAQP4M23) in plasmid pcDNA3.1 (generated as described previously [22]) using Lipofectamine 2000 (Invitrogen) according to manufacturer's instructions. Stable transformants were selected with 500 μg/mL G418 (Invitrogen). Resistant colonies were tested for the expression and cloned. For transient transfections, L-cells were plating onto 6-well plates and transfected with Lipofectamine 2000. Experiments were done 48 hr after transfection. Mouse E-cadherin cDNA in pSTEM1 was provided by Dr. Masatoshi Takeichi (Riken Institute, Japan). Stably transfected CHO-K1 cells (ATCC CCL-61) expressing AQP4 [22, 31] were grown in Ham's nutrient mix supplemented with 10% fetal calf serum at 37 °C in 5% CO_2. The clonal cell populations expressed AQP4 protein strongly in their plasma membranes and were highly water permeable. Astroglia were cultured from cortex of wildtype and AQP4 null neonatal mice as described [23]. At confluence (day 10), primary astroglia were shaken at 200 rpm for 18 h at 37 °C to remove microglia [34], and 0.15 mM dibutyryl cAMP was added to induce differentiation.

Immunocytochemistry

Cells were fixed with 4% paraformaldehyde for 15 min and then washed with PBS. Cells were blocked with 1% bovine serum albumin (BSA), and incubated with primary 1:200 rabbit anti-AQP4 antibody (Ab) (Millipore) or 1:500 mouse anti-GFAP (Sigma) for 1 hr at room temperature and detected with Texas Red-conjugated goat anti-rabbit or FITC-conjugated goat anti-mouse secondary antibodies (1:200 for both; Jackson ImmunoResearch Laboratories, Inc.). Nuclei were counterstained blue with 4,6-diamidino-2-phenylindole (DAPI). Sections were visualized on an inverted fluorescence microscope equipped with a high-resolution Spot color cooled CCD camera (Diagnostic Instruments, Sterling Heights, MI).

Cell aggregation assay

An established cell aggregation assay was used as described [28, 29]. Briefly, to obtain a single cell suspension, cells were incubated with 0.25% trypsin and 1 mM EDTA at 37 °C for 5 min, and dispersed by gentle pipetting. The cells were then suspended in Hanks balanced salt solution (10^6 cells/ml), placed in 24-well plates pre-coated with 2% BSA, and rotated on a orbital shaker (80 rpm) at 37 °C for specified periods of time. An equal volume of 2% glutaraldehyde was added to prevent further aggregation or dissociation of aggregates [30]. The extent of aggregation was determined from the ratio of the total particle number at time t of incubation (N_t) to the initial particle number (N_0). Particle number was determined by counting representative aliquots on a hemocytometer.

In a related assay, AQP4 wildtype and null astrocytes were separately labeled with CellTracker™ Red CMTPX and CellTracker™ Green CMFDA (Invitrogen). Cells were incubated with dyes (2 μM) in Opti-MEM for 30 min, washed 2 times with Opti-MEM,

incubated for 1 h in DMEM, and suspended as above in HBSS. Cells were mixed at a 1:1 ratio and incubated as described above. Green and red fluorescence images were obtained of particles/aggregates after deposition on a coverglass using a Nikon 2000 epifluorescence microscope. In some experiments, aggregation was measured in Ca^{2+}/Mg^{2+}-free HBSS containing 10 mM EDTA.

Peptide association studies

Astrocytes or CHO cells were seeded on the BD Falcon™ 8-well CultureSlides (Fisher Scientific, Pittsburgh, PA) until confluence. A peptide (NH_2- PPSVVGGLG-COOH) containing amino acid residues 139-142 of AQP4 was synthesized with or without an N-terminus fluorescein label (Sigma Genosys). 100 μL of HBSS containing different concentrations of the fluorescent peptide (1–500 μM) was added in each well and incubated at room temperature for 30 min, 2% glutaraldehyde was then added to prevent dissociation of bound peptide, and cells were washed with PBS. Experiments were also done with a large excess of unlabeled peptide included with the fluorescent peptide. Cell-associated fluorescence was determined by quantitative image analysis.

Vesicle aggregation assay

Plasma membrane vesicles were isolated from control and AQP4-expressing CHO-K1 cells by sucrose gradient centrifugation as described [22]. Cells from five 25-cm diameter plastic dishes were grown to confluence (1–3 x 10^8 cells/dish), released by agitation in PBS containing 10 mM EGTA, and washed twice (100 x g, 10 min) at 4 °C in homogenizing buffer (HB, 250 mM sucrose, 10 mM Tris-HCl, pH 7.4). The pellet was resuspended in HB containing antipain (1 μg/ml), pepstatin (1 μg/ml) and benzamidine (15 μg/ml), and homogenized by 20 strokes of a glass Dounce homogenizer. The homogenate was centrifuged at 500 x g for 10 min at 4 °C and adjusted to 1.4 M sucrose, 10 mM Tris-HCl, 0.2 mM EDTA (pH 7.4). A discontinuous sucrose gradient (2 M sucrose (2.5 ml), 1.6 M (5 ml), 1.4 M (10 ml, containing homogenate), 1.2 M (10 ml), 0.8 M (2.5 ml)) was centrifuged for 2.5 h at 25,000 rpm in an SW 28 rotor, and 5 ml fractions were collected. After centrifugation (25,000 rpm, 30 min), the plasma membrane vesicles were resuspended using a 30-gauge needle in 100 μL HB buffer or HBSS, and shaken overnight at 4 °C. Aggregation was stopped by addition of an equal volume of 2% glutaraldehyde. Vesicle diameter was determined by quasi-elastic light scattering using a Zetasizer (Malvern Instruments, Inc., Southborough, MA). The intensity of the laser light scattered by the samples was detected at an angle of 90°. Vesicle size distributions were determined by autocorrelation analysis using Malvern software.

Immunoblot analysis

L-cells were harvested and homogenized in 250 mM sucrose, 1 mM EDTA, 2 μg/ml aprotinin, 2 μg/ml pepstatin A, 2 μg/ml leupeptin, and 100 μg/ml serine protease inhibitor (Sigma). Homogenates were centrifuged at 500 x g for 5 min and the supernatant was collected and stored at −80 °C. Protein concentration was measured using the Protein Assay Kit II (Bio-Rad Laboratories, Hercules, CA). Proteins were electrotransferred to a polyvinylidene difluoride membrane and incubated with rabbit anti-AQP4 (1:1000, Chemicon) or anti-β-actin antibody (1:2000, GE Healthcare, Piscataway, NJ) followed by horseradish peroxidase-linked anti-rabbit IgG (1:10.000, GE Healthcare), and visualized by enhanced chemiluminescence (Roche Diagnostics, Indianapolis, IN).

Acknowledgments

We appreciate the gift of mouse E-cadherin cDNA from Dr. Masatoshi Takeichi (Riken Institute, Japan) and thank Drs. Zhaohua Huang and Francis C. Szoka for assistance in quasi-elastic light scattering measurements. This study

was supported by NIH grants DK35124, EY13574, HL73856, EB00415, HL59198 and DK72517, and grants from the Cystic Fibrosis Foundation.

References

1. Verkman AS, Binder DK, Bloch O, Auguste K, Papadopoulos MC. Three distinct roles of aquaporin-4 in brain function revealed by knockout mice. Biochim Biophys Acta. 2006; 1758:1085–93. [PubMed: 16564496]
2. Bloch O, Auguste KI, Manley GT, Verkman AS. Accelerated progression of kaolin-induced hydrocephalus in aquaporin-4-deficient mice. J Cereb Blood Flow Metab. 2006; 26:1527–37. [PubMed: 16552421]
3. Papadopoulos MC, Verkman AS. Aquaporin-4 gene disruption in mice reduces brain swelling and mortality in pneumococcal meningitis. J Biol Chem. 2005; 280:13906–12. [PubMed: 15695511]
4. Papadopoulos MC, Manley GT, Krishna S, Verkman AS. Aquaporin-4 facilitates reabsorption of excess fluid in vasogenic brain edema. Faseb J. 2004; 18:1291–3. [PubMed: 15208268]
5. Manley GT, Fujimura M, Ma T, Noshita N, Filiz F, Bollen AW, Chan P, Verkman AS. Aquaporin-4 deletion in mice reduces brain edema after acute water intoxication and ischemic stroke. Nat Med. 2000; 6:159–63. [PubMed: 10655103]
6. Auguste KI, Jin S, Uchida K, Yan D, Manley GT, Papadopoulos MC, Verkman AS. Greatly impaired migration of implanted aquaporin-4-deficient astroglial cells in mouse brain toward a site of injury. Faseb J. 2007; 21:108–16. [PubMed: 17135365]
7. Saadoun S, Papadopoulos MC, Watanabe H, Yan D, Manley GT, Verkman AS. Involvement of aquaporin-4 in astroglial cell migration and glial scar formation. J Cell Sci. 2005; 118:5691–8. [PubMed: 16303850]
8. Papadopoulos MC, Saadoun S, Verkman AS. Aquaporins and cell migration. Pflugers Arch. 2008; 456:693–700. [PubMed: 17968585]
9. Lu DC, Zhang H, Zador Z, Verkman AS. Impaired olfaction in mice lacking aquaporin-4 water channels. Faseb J. 2008 in press.
10. Binder DK, Yao X, Zador Z, Sick TJ, Verkman AS, Manley GT. Increased seizure duration and slowed potassium kinetics in mice lacking aquaporin-4 water channels. Glia. 2006; 53:631–6. [PubMed: 16470808]
11. Padmawar P, Yao X, Bloch O, Manley GT, Verkman AS. K+ waves in brain cortex visualized using a long-wavelength K+-sensing fluorescent indicator. Nat Methods. 2005; 2:825–7. [PubMed: 16278651]
12. Li J, Patil RV, Verkman AS. Mildly abnormal retinal function in transgenic mice without Muller cell aquaporin-4 water channels. Invest Ophthalmol Vis Sci. 2002; 43:573–9. [PubMed: 11818406]
13. Li J, Verkman AS. Impaired hearing in mice lacking aquaporin-4 water channels. J Biol Chem. 2001; 276:31233–7. [PubMed: 11406631]
14. Binder DK, Papadopoulos MC, Haggie PM, Verkman AS. In vivo measurement of brain extracellular space diffusion by cortical surface photobleaching. J Neurosci. 2004; 24:8049–56. [PubMed: 15371505]
15. Hiroaki Y, Tani K, Kamegawa A, Gyobu N, Nishikawa K, Suzuki H, Walz T, Sasaki S, Mitsuoka K, Kimura K, Mizoguchi A, Fujiyoshi Y. Implications of the aquaporin-4 structure on array formation and cell adhesion. J Mol Biol. 2006; 355:628–39. [PubMed: 16325200]
16. McCoy E, Sontheimer H. Expression and function of water channels (aquaporins) in migrating malignant astrocytes. Glia. 2007; 55:1034–43. [PubMed: 17549682]
17. Fotiadis D, Hasler L, Muller DJ, Stahlberg H, Kistler J, Engel A. Surface tongue-and-groove contours on lens MIP facilitate cell-to-cell adherence. J Mol Biol. 2000; 300:779–89. [PubMed: 10891268]
18. Hasler L, Walz T, Tittmann P, Gross H, Kistler J, Engel A. Purified lens major intrinsic protein (MIP) forms highly ordered tetragonal two-dimensional arrays by reconstitution. J Mol Biol. 1998; 279:855–64. [PubMed: 9642066]

19. Engel A, Fujiyoshi Y, Gonen T, Walz T. Junction-forming aquaporins. Curr Opin Struct Biol. 2008; 18:229–35. [PubMed: 18194855]
20. Nagafuchi A, Shirayoshi Y, Okazaki K, Yasuda K, Takeichi M. Transformation of cell adhesion properties by exogenously introduced E-cadherin cDNA. Nature. 1987; 329:341–3. [PubMed: 3498123]
21. Yang B, Zhang H, Verkman AS. Lack of aquaporin-4 water transport inhibition by antiepileptics and arylsulfonamides. Bioorg Med Chem. 2008 in press.
22. Yang B, Brown D, Verkman AS. The mercurial insensitive water channel (AQP-4) forms orthogonal arrays in stably transfected Chinese hamster ovary cells. J Biol Chem. 1996; 271:4577–80. [PubMed: 8617713]
23. Solenov E, Watanabe H, Manley GT, Verkman AS. Sevenfold-reduced osmotic water permeability in primary astrocyte cultures from AQP-4-deficient mice, measured by a fluorescence quenching method. Am J Physiol Cell Physiol. 2004; 286:C426–32. [PubMed: 14576087]
24. Furman CS, Gorelick-Feldman DA, Davidson KG, Yasumura T, Neely JD, Agre P, Rash JE. Aquaporin-4 square array assembly: opposing actions of M1 and M23 isoforms. Proc Natl Acad Sci U S A. 2003; 100:13609–14. [PubMed: 14597700]
25. Sakisaka T, Takai Y. Cell adhesion molecules in the CNS. J Cell Sci. 2005; 118:5407–10. [PubMed: 16306219]
26. Walsh FS, Doherty P. Neural cell adhesion molecules of the immunoglobulin superfamily: role in axon growth and guidance. Annu Rev Cell Dev Biol. 1997; 13:425–56. [PubMed: 9442880]
27. Chothia C, Jones EY. The molecular structure of cell adhesion molecules. Annu Rev Biochem. 1997; 66:823–62. [PubMed: 9242926]
28. Satoh-Horikawa K, Nakanishi H, Takahashi K, Miyahara M, Nishimura M, Tachibana K, Mizoguchi A, Takai Y. Nectin-3, a new member of immunoglobulin-like cell adhesion molecules that shows homophilic and heterophilic cell-cell adhesion activities. J Biol Chem. 2000; 275:10291–9. [PubMed: 10744716]
29. Hirano S, Yan Q, Suzuki ST. Expression of a novel protocadherin, OL-protocadherin, in a subset of functional systems of the developing mouse brain. J Neurosci. 1999; 19:995–1005. [PubMed: 9920663]
30. Takeichi M. Functional correlation between cell adhesive properties and some cell surface proteins. J Cell Biol. 1977; 75:464–74. [PubMed: 264120]
31. Farinas J, Kneen M, Moore M, Verkman AS. Plasma membrane water permeability of cultured cells and epithelia measured by light microscopy with spatial filtering. J Gen Physiol. 1997; 110:283–96. [PubMed: 9276754]
32. Kanemaru K, Okubo Y, Hirose K, Iino M. Regulation of neurite growth by spontaneous Ca^{2+} oscillations in astrocytes. J Neurosci. 2007; 27:8957–66. [PubMed: 17699677]
33. Crane JM, Van Hoek AN, Skach WR, Verkman AS. Aquaporin-4 Dynamics in Orthogonal Arrays in Live Cells Visualized by Quantum Dot Single Particle Tracking. Mol Biol Cell. 2008 (in press).
34. Giulian D, Baker TJ. Characterization of ameboid microglia isolated from developing mammalian brain. J Neurosci. 1986; 6:2163–78. [PubMed: 3018187]

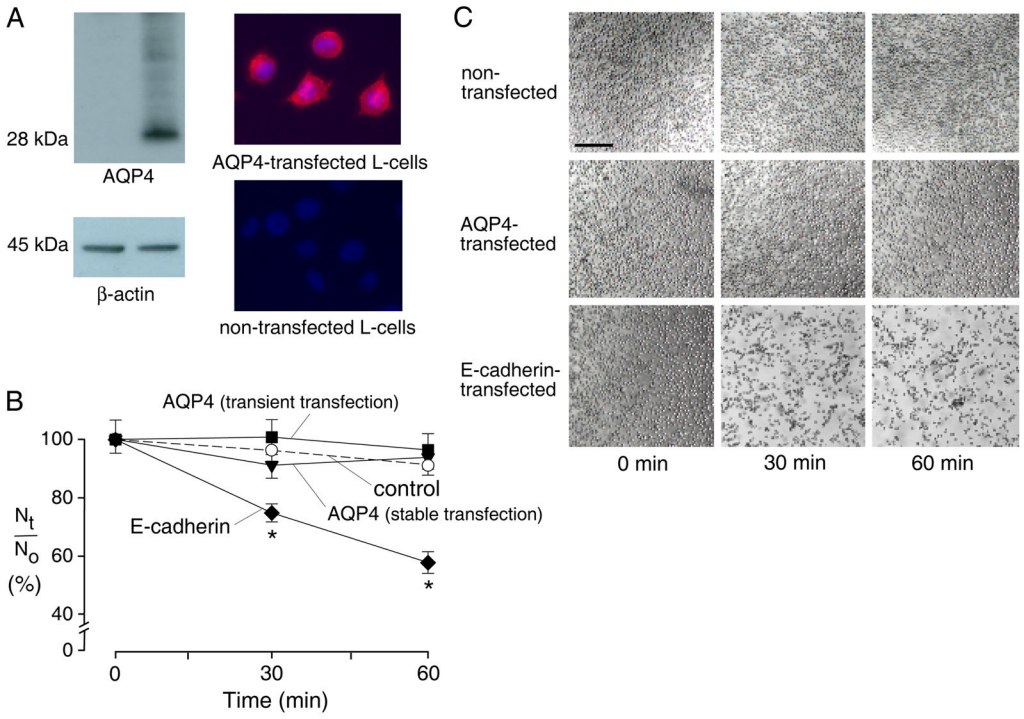

Figure 1. AQP4 expression in L-cells does not increase cell-cell adhesion

A. Immunoblot (left) and immunofluorescence (right) of non-transfected and AQP4 stably transfected L-cells. B. Cell aggregation activity. Self-adhesion of L-cells in single cell suspension measured by counting the number of particles (isolated cells + aggregates) at 0, 30 and 60 min (S.E. n=6 independent experiments). N_t/N_o is the ratio of number of particles at time t vs. time 0. Differences not significant between non-transfected and AQP4-expressing cells. Transient transfection with E-cadherin induced significant aggregation (* $P < 0.01$) compared to non-transfected cells. C. L-cell adhesion assessed by phase-contrast microscopy in which cell suspensions were allowed to settle onto coverglass after terminating aggregation by glutaraldehyde. Few non-transfected and AQP4-expressing cells were adherent, whereas many E-cadherin-transfected cells formed large aggregates. Bar, 100 μm.

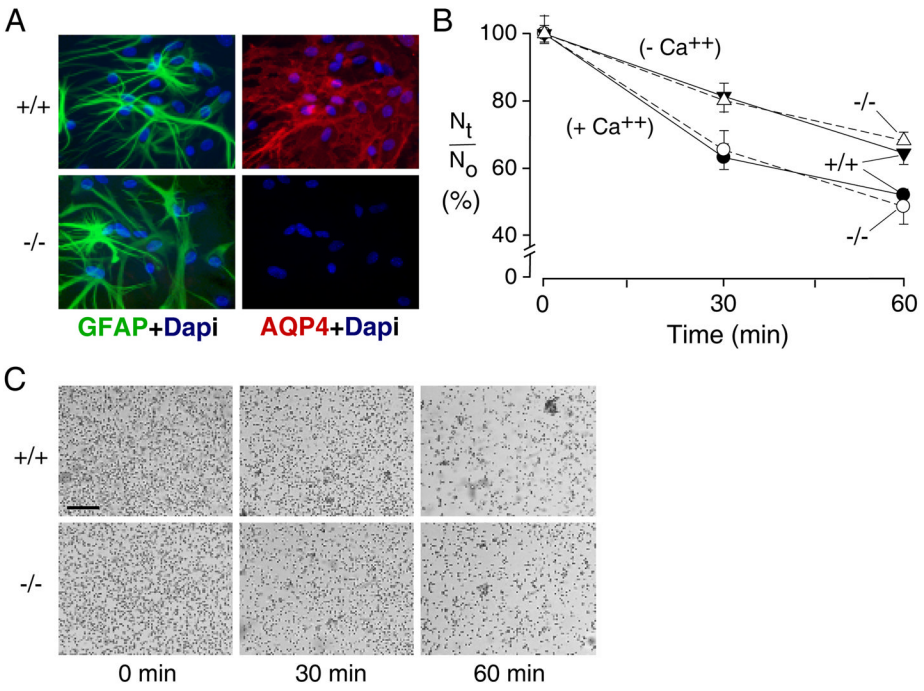

Figure 2. AQP4–independent adhesion in brain glial cells

A. Immunofluorescence showing ~95% of GFAP-positive cells with membrane AQP4 staining in wildtype glial cells. B. Cell-cell adhesion measured as in Fig. 1 for differentiated primary cultures of glial cells from neonatal brains of wildtype and AQP4 null mice (S.E. n=6 independent experiments). Suspensions contained standard HBSS (+ Ca^{++}) or Ca^{2+}/Mg^{2+}-free HBSS containing 10 mM EDTA (− Ca^{++}). Differences not significant between wildtype vs. AQP4-deficient glial cells. C. Phase-contrast micrographs of glial cells after settling on culture plate as in Fig. 1C. Arrows indicate cell aggregates. Bar, 100 μm.

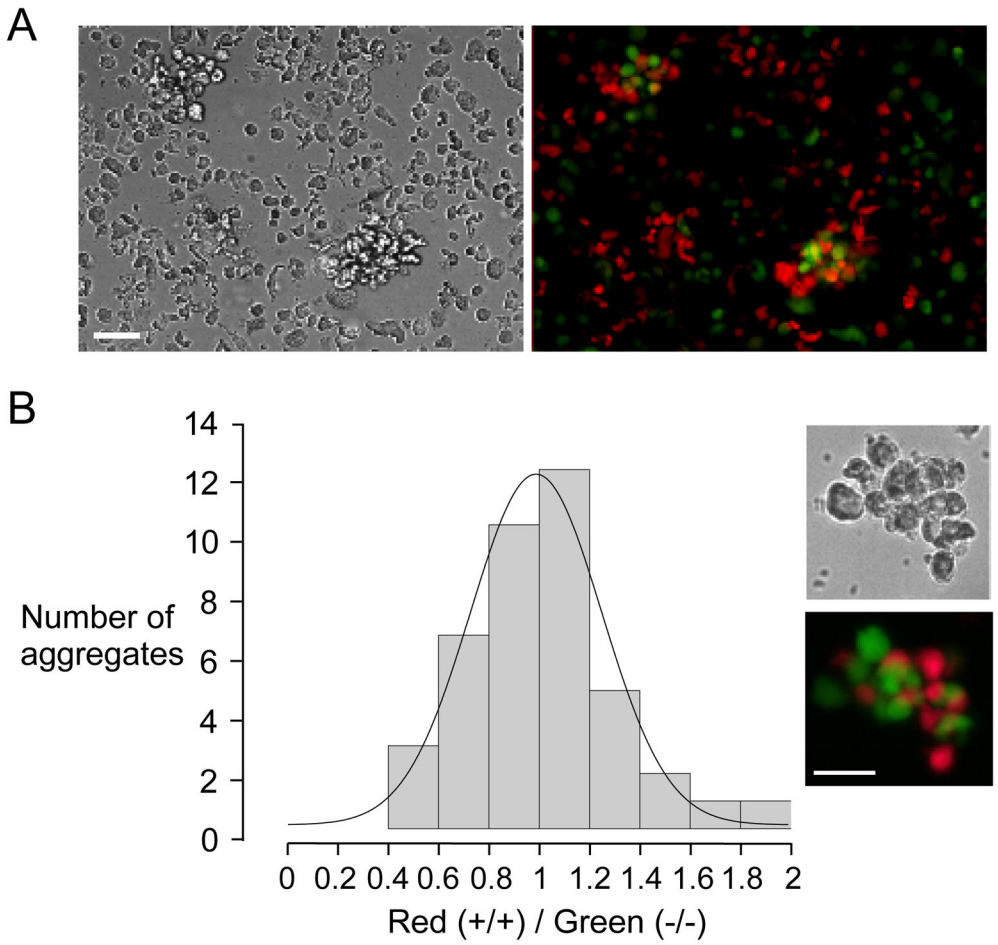

Figure 3. Two-color fluorescence clustering assay of glial cell adhesion

Glial cells were fluorescently stained red (wildtype) and green (AQP4 null). Cell suspensions contained equal numbers of wildtype and AQP4 null cells. A. Representative low magnification phase-contrast (left) and fluorescence (right) micrographs of cells after 30 min in stirred suspension. Bar, 50 μm. B. Histogram of the ratio of red-to-green cells in aggregates, with a total of 39 aggregates counted (range 6 to 24 cells per aggregate). Inset shows example of aggregate at high magnification.

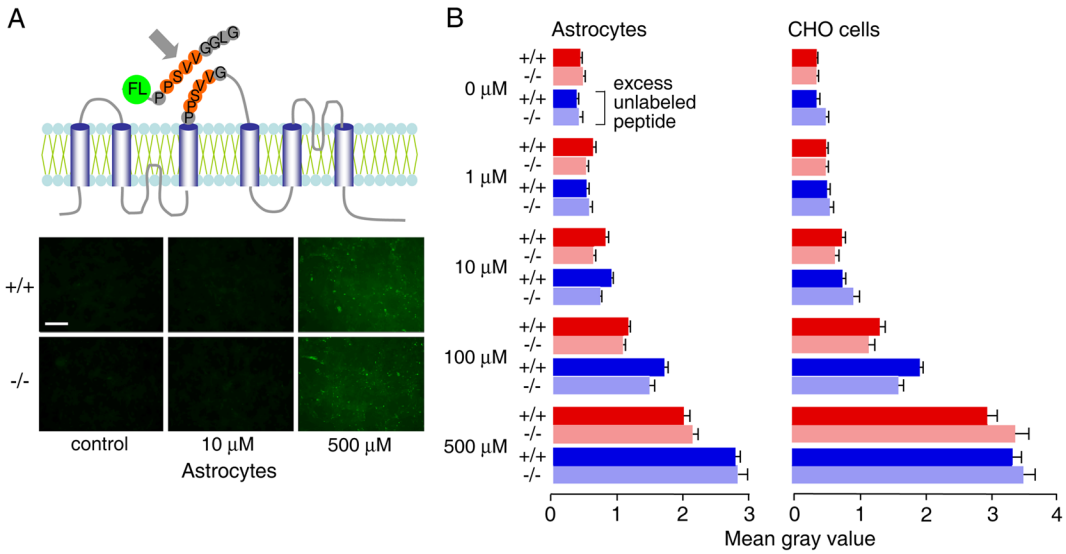

Figure 4. Lack of specific AQP4 binding of a putative AQP4 adhesion oligopeptide

A. (top) Schematic of AQP4 membrane topology showing putative adhesion sequence (residues 139-142) in extracellular loop. The synthetic fluorescein-labeled 9-mer peptide (NH_2-PPSVVGGLG-COOH) is shown. (bottom) Fluorescence micrographs of confluent astrocytes after incubation with indicated concentration of fluorescein-labeled 9-mer peptide for 30 min at room temperature, followed by brief fixation with 2% glutaraldehyde and washing. C. Summary of relative (background-subtracted) cell fluorescence for incubations done at indicated concentrations of the fluorescein-labeled 9-mer peptide, in the absence or presence of 50-fold excess unlabeled peptide (S.E., n=3–4). Differences not significant comparing AQP4 expressing vs. non-expressing glial and CHO cells. +/+: AQP4-expressing cells, −/− AQP4 null cells.

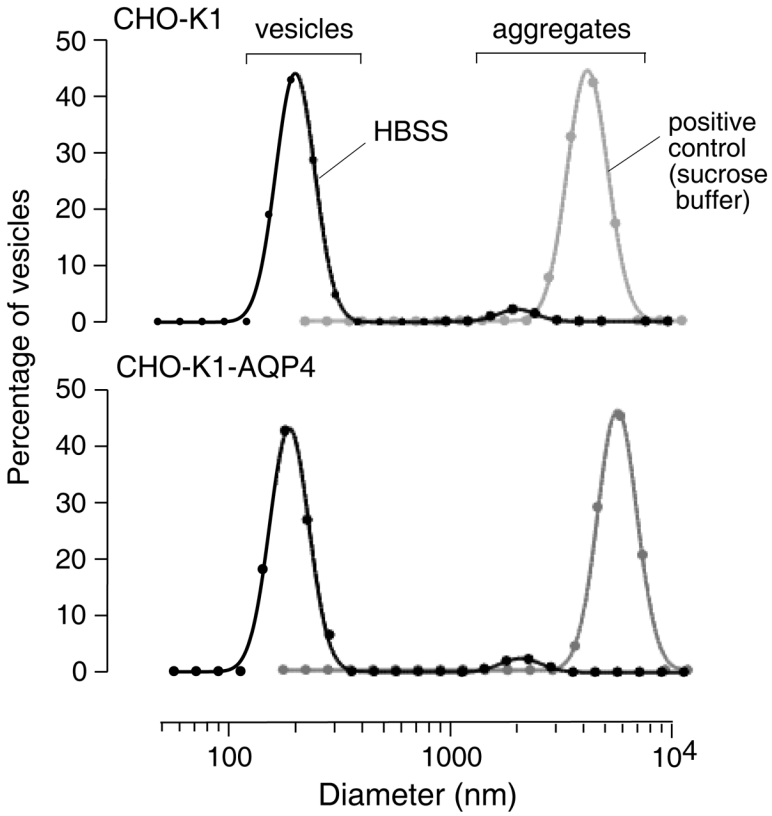

Figure 5. Quasi-elastic light scattering assay of plasma membrane vesicle aggregation

Plasma membrane vesicles isolated from AQP4 expressing and non-expressing CHO-K1 cells were incubated at high density overnight in HBSS. Cell size distributions were measured by quasi-elastic light scattering. Differences not significant in the fraction of aggregates of AQP4-containing vs. control vesicles. As positive control, vesicles were incubated in a low-ionic strength isosmolar sucrose solution to induce aggregation.